ELSEVIER

Tectonophysics 350 (2002) 283–298

TECTONOPHYSICS

www.elsevier.com/locate/tecto

Evaluating magnetic lineations (AMS) in deformed rocks

Josep M. Parés*, Ben A. van der Pluijm

Department of Geological Sciences, University of Michigan, 2534 C. C. Little Building, Ann Arbor, MI 48109, USA

Received 17 October 2001; accepted 1 March 2002

Abstract

Magnetic lineation in rocks is given by a cluster of the principal axes of maximum susceptibility (K_{max}) of the Anisotropy of Magnetic Susceptibility (AMS) tensor. In deformed rocks, magnetic lineations are generally considered to be the result of either bedding and cleavage intersection or they parallel the tectonic extension direction in high strain zones. Our AMS determinations, based on a variety of samples that were taken from mudstones, slates and schists from the Pyrenees and Appalachians, show that strain is not the only factor controlling the development of magnetic lineation. We find that the development and extent to which the magnetic lineation parallels the tectonic extension direction depends on both the original AMS tensor, which in turn depends on the lithology, and the deformation intensity. Rocks having a weak pre-deformational fabric will develop magnetic lineations that more readily will track the tectonic extension.

Keywords: Rock fabrics; Rock magnetism; Anisotropy of Magnetic Susceptibility; Cleavage

1. Introduction

Rock fabrics can reflect the strain state of rocks and are a rich source on information of tectonic evolution. Lineation is a common fabric element in rocks and is particularly useful in deciphering the history of deformation. Lineation is commonly defined as any linear feature that occurs penetratively in a rock and includes form lineations (crenulation, rods, elongate pebbles) and mineral elongation (stretched grains, linear aggregates of equidimensional grains, subhedral grains with an elongate crystal shape, etc.); for a recent review on terminology of lineation, see Piazolo and Passchier (2002). Despite numerous studies, interpreting the significance of lineation in rocks is not straightforward. While some lineations reflect strain axes or kinematic trajectories, others appear to have little kinematic significance. In tranpressional regimes, for example, Tikoff and Greene (1997) conclude that the stretching lineation does not necessarily correlate with the direction of simple shear component of deformation and that it can be either parallel or perpendicular to the shear zone. In some shear zones, lineations that are perpendicular to the flow direction are common, which might suggest that the dominant lineation formed is not a stretching lineation (Tikoff and Greene, 1997). Recently, it has been suggested that the development of lineation is largely a function of the ratio of initial to dynamically recrystallized grain size (Piazolo and Passchier, 2002).

Lineation introduces an anisotropy in the physical properties of rocks and, therefore, it can be deter-

* Corresponding author. Fax: +1-734-763-4690.
E-mail address: jmpares@umich.edu (J.M. Parés).

0040-1951/02/$ - see front matter
PII: S0040-1951(02)00119-1

mined by methods capable of sensing rock anisotropy. Rock anisotropy depends mostly on crystallographic preferred orientation, compositional layering, distribution and size of microfractures, or the shape fabric of grains. The spatial and geometrical configuration of rock components is well assessed by Anisotropy of Magnetic Susceptibility (AMS) studies. AMS in most pelitic rocks represents a measure of the crystallographic orientation of phyllosilicates and other tabular grains and, to a lesser extent, of the grain shape orientation of ferrimagnetic grains (like magnetite). AMS can be represented as an ellipsoid (Nye, 1957), whose semi-axes are the three principal susceptibilities (maximum, intermediate and minimum susceptibility axes, or K_{max}, K_{int} and K_{min} hereafter). Many workers consider that AMS axes orientations typically show a one-to-one correlation with the principal strain directions (see reviews by Hrouda, 1982; Borradaile, 1987, 1991; Borradaile and Henry, 1997), a view that has prevailed for almost two decades. Nevertheless,

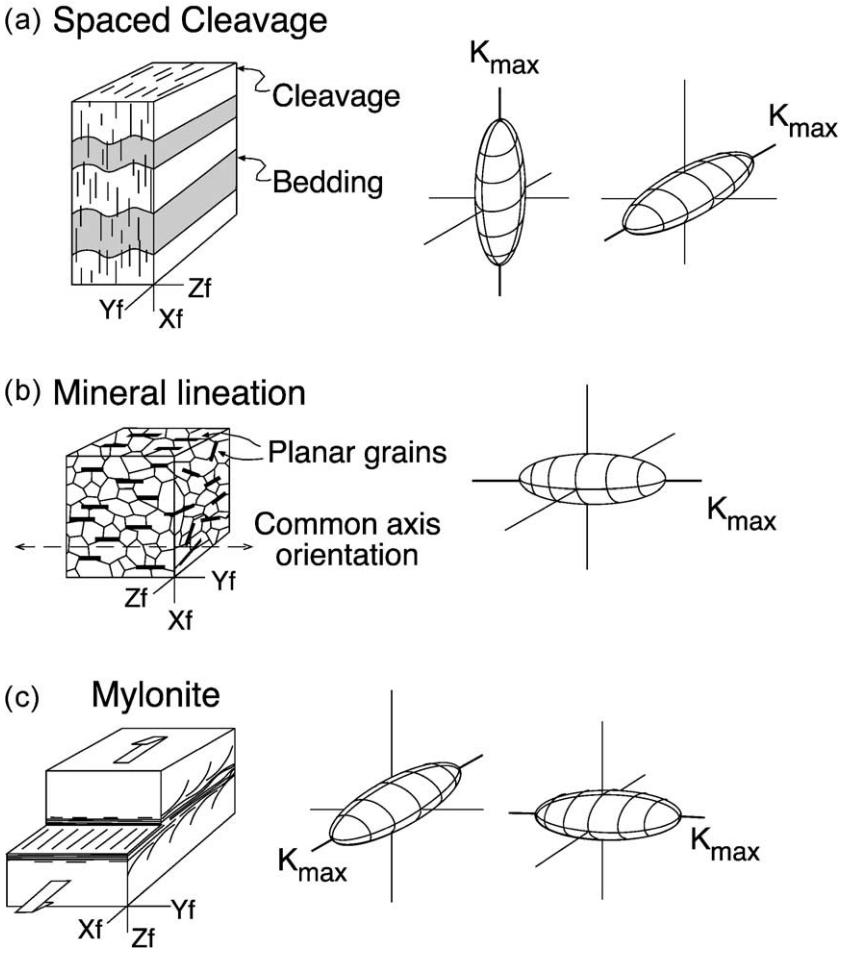

Fig. 1. Diagrammatic representation of various type of magnetic lineation in deformed rocks. X_f, Y_f, Z_f are the orientations of the finite strain ellipsoid. (a) Spaced and slaty cleavage. Magnetic lineation will be given by either the intersection direction of bedding and cleavage or by the extension direction within the cleavage plane (in the example, it is supposed to be vertical). It is assumed that microlithons are smaller than the volume of the measured sample. (b) Mineral lineation defined by euhedral or subhedral planar grains (such as micas) that share a common axis. In this situation, magnetic lineation will track the intersection axes of the planar grains. (c) Mylonite zones produce a magnetic lineation that is either parallel or perpendicular to the stretching lineation, or in between.

numerical and experimental models (e.g. Borradaile, 1988; Housen et al., 1993) reveal that some components, specifically magnetic lineation (L_m), as given by a cluster of K_{max} axes, is often determined by the interaction of two fabrics; that is, L_m parallels the intersection of two competing sub-fabrics. Studies in naturally and artificially deformed sediments indeed show that L_m often tracks the intersection direction of two planar fabrics (Borradaile and Tarling, 1981; Richter et al., 1993). In many other cases, however, L_m orientation tracks the bulk extension direction X (e.g. Kligfield et al., 1981; Ferré and Améglio, 2000; Hirt et al., 2000) or, as shown in this paper, has intermediate orientations. Specifically, in deformed pelitic rocks, the magnetic lineation has been observed to parallel either the stretching direction (e.g. Lamarche and Rochette, 1987; Hirt et al., 2000) or the intersection of bedding and cleavage planes (e.g. Borradaile and Tarling, 1981; Rochette and Vialon, 1984; Parés and Dinarès, 1993). The most obvious means of determining the origin of magnetic lineation in deformed rocks is to obtain AMS records from rocks deformed in different tectonic environments in order to compare the magnetic anisotropy tensor and its axes distribution with the structural elements.

Fig. 1 summarizes three possible scenarios of magnetic lineation development as produced in three different deformation environments. In this paper, we explore the significance of the L_m in rocks with different deformation intensity to further understanding the relationship between tectonic and magnetic lineations in deformed rocks.

2. Magnetic lineation in deformed rocks

First, we will discuss the properties of magnetic fabrics and, specifically, the magnetic lineation in deformed rocks. We examine the AMS in two end member environments, sedimentary rocks and mylonites.

A variety of experimental and observational approaches have led to an understanding of magnetic lineation development in deformed sedimentary rocks. One of the earliest realizations is that under very low deformation intensity, a magnetic lineation can develop parallel to fold axes. Such a feature was first reported by Kissel et al. (1986) while investigating marine Cenozoic clays in Greece. Grouping of K_{max} under progressive deformation has been observed in later studies, and is occasionally accompanied by a girdle containing K_{min} and K_{int} axes. This particular axes distribution is thought to be the first evidence for layer parallel shortening in sedimentary rocks, as noticed by Sagnotti and Speranza (1993), Parés and Dinarès (1993), Sagnotti et al. (1994) and Parés et al. (1999) in sequences of low to moderately deformed mudstones. In the same line of observation, experimental and numerical models by Housen et al. (1993) illustrate that when two planar mineral fabrics contribute to the mean AMS tensor, the intersection of these two sub-fabrics will control the orientation of the K_{max} direction, as previously pointed by Borradaile (1988). Moreover, in higher deformation intensity environments, a similar sequence from bedding to tectonic fabric is observed (Borradaile and Tarling, 1981; Kligfield et al., 1981; Housen and van der Pluijm, 1990, 1991). Collectively, regardless of strain history, these observations document the change in magnetic anisotropy from a primary (sedimentary) fabric to a tectonic fabric.

The commonly observed situation where K_{max} is parallel to the intersection lineation has been classically interpreted as an intermediate deformation stage that eventually will led to an "idealized" tectonic AMS relation, where $X \| K_{max}$, $Y \| K_{int}$ and $Z \| K_{min}$ (Borradaile and Henry, 1997; Borradaile and Tarling, 1981). According to this scenario, K_{max} becomes parallel to bedding–cleavage intersection, but will progress to parallelism with the tectonic extension direction by progressive deformation when the tectonic AMS tensor completely overprints the primary fabric. This implies that the development and extent to which K_{max} parallels the X-strain, axis mostly depend on deformation intensity, and that the magnetic lineation has thus the potential to track the bulk strain ellipsoid. We will return to this point in a later section.

Magnetic anisotropy methods have also been successfully applied to the study of shear zones and mylonites, which often lack conventional strain markers and have textures that are difficult to quantify (Goldstein, 1980; Goldstein and Brown, 1988; Ruf et al., 1988; Housen et al., 1995). In many cases, the orientation of the L_m tracks mineral elongation lineations as measured in the field (e.g. Aranguren et al., 1996), however, in the Pinaleno Mountains metamor-

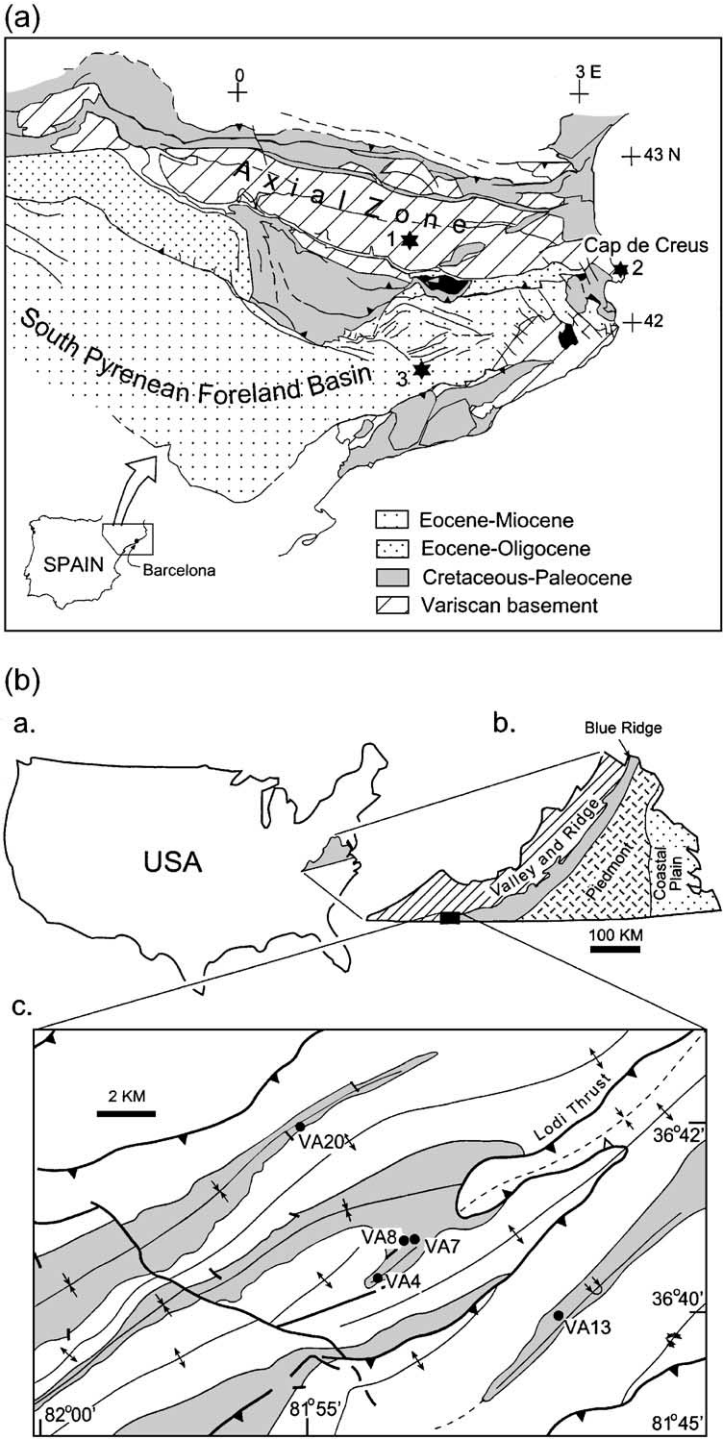

Fig. 2. Geological setting of the studied areas. (a) Pyrenees. Stars denote the location of the sample localities: 1—PYR (Variscan basement), 2—CDC (Variscan basement, shear zones), 3—FE (Pyrenean Foreland Basin). (b) SW Appalaches, SW Virginia (modified from Reks and Gray, 1982).

phic complex (Arizona), a mylonite zone studied by Ruf et al. (1988), the maximum susceptibility axes do not parallel the maximum extension direction. In this case, the minimum susceptibility direction coincides with the mylonitic foliation pole, but K_{max} and K_{int} do not coincide with the X and Y strain axes, respectively. Thus, the relationship between the orientation of magnetic and tectonic lineation in deformed rocks is variable, with L_m reflecting either an intersection lineation, the extension direction or an orientation in between. Here we present new results from naturally deformed rocks with different deformation intensity in order to examine the significance of magnetic lineation in rocks as an indicator of deformation state.

3. Approach and methods

To explore the development of magnetic lineation in rocks with varying strain, we selected deformed rocks from various localities within the Pyrenean and the Appalachian orogenic belts that represent distinct strain environments (Fig. 2). All AMS measurements for this study were carried out with a susceptibility bridge, Kappabridge KLY-2.03 (Geofyzika Brno, now AGICO), measuring fifteen directional susceptibilities on a frequency of 920 Hz (sensitivity of the coil is $\sim 5 \times 10^{-7}$ SI). AMS data analysis has been performed by linear perturbation analysis (LPA, Tauxe, 1998), following the method initially developed by Constable and Tauxe (1990) for statistical bootstrap of anisotropy data to obtain the confidence ellipses. First, the matrix elements and residual error for each individual sample are calculated using the obtained fifteen measurements following the scheme of Jelinek (1978) ('k15_s' program of Tauxe, 1998). Then, we calculate the bootstrap statistics for the matrix elements ('bootams' program of Tauxe, 1998). Instead of plotting the 95% confidence ellipses, which all require unnecessary parametric assumptions (Tauxe, 1998), we use the bootstrap eigenvectors, displayed on a stereonet as a smear of points around the bootstrap eigenparameters. Confidence region for the bootstrapped distributions can be drawn as a contour line enclosing 95% of the bootstrapped eigenvectors. Details on the bootstrap method to assess confidence intervals can be found in Tauxe (1998). Data and results are listed in Table 1, including the eigenvalues for the principal, major and minor eigenvectors and bulk magnetic susceptibility.

Table 1
Summary of the Anisotropy Magnetic Susceptibility data

Site	Rock	τ_1	Dec	Inc	τ_2	Dec	Inc	τ_3	Dec	Inc	K (SI)
CDC1	Schist	0.35979	287.1	35.1	0.35443	26.2	12.6	0.28577	132.8	52.0	358
CDC2	Schist	0.36060	310.3	23.5	0.35735	65.1	43.9	0.28206	201.3	36.8	325
CDC3	Grnte	0.34388	331.7	3.4	0.33492	63.3	24.9	0.32120	234.3	64.9	295
PYR2	Slates	0.49235	288.4	58.5	0.30094	100.5	31.2	0.20671	192.6	3.5	670
PYR3	Slates	0.48086	286.3	58.7	0.31404	104.7	31.3	0.20510	195.2	0.7	830
PYR4	Slates	0.41153	280.7	57.6	0.33175	98.9	32.4	0.25672	189.2	0.8	819
PYR5	Slates	0.41704	291.9	50.2	0.32742	72.4	32.8	0.25554	176.0	20.0	529
PYR6	Slates	0.36369	270.9	57.5	0.33092	58.0	28.1	0.30539	156.2	14.9	315
PYR7	Slates	0.37707	258.5	58.2	0.33121	99.1	30.2	0.29172	3.7	9.2	826
PYR8	Shales	0.38632	357.6	56.5	0.34590	107.9	13.0	0.26778	205.7	30.3	188
FE02	Mdstn	0.34023	91.1	0.1	0.33074	0.9	45.0	0.32903	181.2	45.0	160
FE05	Mdstn	0.33979	267.3	7.9	0.33132	2.7	33.9	0.32889	166.0	54.9	185
FE09	Mdstn	0.33912	88.3	3.2	0.33195	351.3	65.1	0.32893	179.8	24.7	175
FE04	Mdstn	0.33827	284.8	5.4	0.33564	194.0	8.1	0.32608	48.2	80.3	105
FE10	Mdstn	0.33648	262.6	9.2	0.33373	79.5	12.1	0.32979	171.8	5.0	160
VA7	Mdstn	0.34549	248.0	16.9	0.34050	352.7	39.8	0.31401	140.2	45.3	308
VA8	Mdstn	0.34602	59.0	11.0	0.33795	314.6	52.0	0.31603	157.1	35.8	427
VA13	Mdstn	0.34752	61.2	6.3	0.33523	155.3	33.1	0.31725	321.7	56.2	433
VA20	Mdstn	0.34795	235.5	8.4	0.33874	31.7	1.7	0.31332	132.4	57.0	397
VA4	Mdstn	0.34263	65.4	6.0	0.33046	163.5	53.1	0.32191	331.0	36.2	318

τ_i are the eigenvalues and Dec and Inc the associated eigenvectors (mapped to the lower hemisphere). Matrix elements have been calculated from 15 measurements using Jelinek's (1976) scheme, and best-fit tensor elements estimated utilizing Tauxe's (1998) program.

4. Case studied: Pyrenees and Appalachians

The Pyrenean Range extends from the Galician continental margin in the west to the Languedoc–Provence zone in the east, for more than 1000 km and formed during convergence between the Iberian and the European plate in latest Cretaceous to Oligocene times. Typically, the Pyrenees are divided into several structural zones, most of which are bounded by major faults (Fig. 2a). The North Pyrenean Zone includes Mesozoic and Variscan basement, also called the North Pyrenean massifs. The axial zone of the chain is essentially made up of Paleozoic rocks and along with the North Pyrenean massifs constitute the Variscan basement of the Pyrenees, where the study localities (PYR and CDC) are found. During the Variscan orogeny in late Carboniferous times, the Paleozoic rocks were affected by polyphase tectonics and metamorphism.

The Mesozoic and Cenozoic cover of thrusted units are affected by a large southward translation. The South Pyrenean units that are involved in this southward thrusting show typical thin-skin tectonics (Seguret, 1972; Deramond et al., 1985; Muñoz et al., 1986; Choukroune et al., 1989). The décollement zone of the Mesozoic and Cenozoic cover only emerges locally in South Pyrenees, in the mainly undeformed Ebro Molassic southern foreland basin where Tertiary strata rest on the Variscan basement or Mesozoic cover. Well south of the belt in the South Foreland Basin, the subhorizontal Eocene rocks still exhibit a remarkable degree of deformation, of up to about 35% shortening (Casas et al., 1996).

The Massana anticlinorium (sites PYR) (Fig. 2) marks the western edge of a large-scale anticline in the Variscan Central Pyrenees (Zwart, 1979; Poblet, 1991). The anticlinorium extends E–W for about 50 km and is made up of undistinguished Cambrian–Ordovician to Silurian rocks. The region is bounded by two E–W thrust faults that are probably Tertiary in age. The studied Cambrian–Ordovician rocks (sites PYR on Table 1) are composed of a rythmic milimetric or centimetric succession of slates and fine grained sandstones. Overlying this azoic sediments, a succession of conglomerates and sandstones (Ordovician) and slates (Silurian) are found. The structure of the Massana anticlinorium has been explained by the superposition of two folding events (Cirés et al., 1990; Poblet, 1991). The first folding event produced tight to open folds, with E–W trending axial surfaces verging to the North. A second folding event gave rise to a better-developed fold system with South vergence. The last folding event is also responsible for crenulation cleavage, which is the penetrative fabric best developed and most apparent in the area. Crenulation planes are E–W trending and steeply dipping to the north. Both fold axes and intersection lineations of cleavage and bedding show a dispersion on the cleavage plane due to the later folding event. Locally, stretching lineations, given by preferred mineral orientations, plunge to the WNW are observed (Capellà, 1997). All over the Massana anticlinorium area, the crenulation cleavage is the most apparent structure and is the reference plane for the study of younger deformation events. The latter are a system of E–W trending North vergence folds. Most workers of this area agree that both folding events are Variscan, though some Tertiary deformation cannot be ruled out. The development of the crenulation cleavage takes place at very low grade metamorphism, below the chlorite–muscovite zone.

The Cap de Creus region is the easternmost late Variscan outcrop in the Axial Zone of the Pyrenees (Fig. 2a). Both metasediments and granites of presumed Upper Ordovician age have been affected by post-intrusive deformation (Carreras et al., 1977; Simpson, 1983; Carreras and Druguet, 1994). This deformation is thought to be of late Carboniferous age and is produced by ductile and britle–ductile shear zones. A first cleavage is subparallel to bedding and developed prior to the metamorphic peak. The last major deformational event gave rise to E–W and NW–SE trending shear zones that developed under greenschist and lower amphiboliote facies conditions (Carreras et al., 1977; Druguet et al., 1997). These shear zones form an anastomosing three-dimensional network, leading to the isolation of variably sized rhomb-shaped domains of rocks not affected by mylonitization. The sequence of deformation events in the Roses granodiorite began with the formation of a weak linear and planar fabric by dynamic recrystallization of constituent minerals under upper greenschist facies conditions (Simpson et al., 1982). This event was followed by the formation of an anastomosing network of ductile

shear zones, centimeters to tens of meters in width. These later conditions favored deformation of feldspar, quartz and mica by microfracturing and crystal plasticity. In outcrop, two distinct orientations of fabric can be discerned in the shear zone (Simpson, 1983): A foliation that is inclined at 30–40° to the shear zone boundaries and discrete slip surfaces that are roughly parallel to the shear zone boundaries.

In the South Pyrenean Foreland Basin, the base of the Tertiary beds in the Ebro Basin is very shallow in the southern part of the basin, and over 5000 m deep in the northern part. From the uppermost Cretaceous to the late Eocene, the main trough of the southern foreland was connected to the Atlantic Ocean, giving rise to widespread marine deposition. A rapid Middle to Late Eocene transgression occurred leading to a thick marine sequence, during which the mudrocks used in the present study were deposited. The Eocene mudrocks are flat lying across most the Pyrenean Foreland Basin, and seemingly undeformed, but they are involved in the Southern Pyrenean Range along the northern rim of the Foreland Basin.

Localities that were sampled in the Appalachian Valley and Ridge Province of the USA include weakly deformed mudstones that belong to the Knobs Formation (Fig. 2b). These rocks show well-developed pencil structure, which focuses on the intermediate stages between sedimentary and tectonic fabrics (Reks and Gray, 1982). The Knobs Formation extends in the Southern Appalachian fold and thrust foreland (Valley and Ridge Province) in southwestern Virginia. This portion of the Appalachian belt is characterized by long, linear and arcuate NE–SW trending thrust faults. Some of the faults truncate regional anticlines and synclines. Reks and Gray (1982) described pencil development in weakly deformed siltstone and mudstones in the Middle Ordovician Knobs Fm, which we have resampled for magnetic fabric study.

5. Magnetic fabric data

5.1. Paleozoic shales (sites PYR)

The principal axes of susceptibility of the PYR slates typically cluster and produce well defined ellipsoids. Generally, K_{max} axes group around a WNW and moderately shallow direction (Fig. 3). The principal axes of maximum susceptibility K_{max} plunge on average 283/58 and do not coincide with the intersection lineation of cleavage and bedding (Casas et al., 1998). It is apparent from the stereonet projection that the principal axes of K_{min} parallel the pole to cleavage orientation. Site PYR8 (Fig. 3c) is the only where a stretching lineation was observed, and here the magnetic lineation parallels the stretching direction and not the bedding–cleavage intersection.

5.2. Cap de Creus mylonites (sites CDC)

Low-grade metamorphic Ordovician schists are locally deformed in ductile shear zones that developed a mylonitic cleavage. The rocks have a regional cleavage striking NE–SW and dipping to the NW, whereas in shear zones, a NW–SE mylonitic foliation develops. The schists have a well-developed magnetic fabric that is consistent with the regional cleavage, with K_3 axes normal to cleavage and K_{max} axes plunging to the NW within the foliation plane (Fig. 4a). The magnetic foliation (planes containing K_{int}–K_{max}) tracks the regional cleavage. In the shear zone, where strain is much higher, the situation is quite different (Fig. 4b). Here, K_{min} axes of mylonitized schists are normal to the foliation, yet K_{max} axes cluster around the intersection of the regional cleavage and the mylonitic foliation. The magnetic fabrics in the shear zone provide an example of magnetic lineation that is parallel to the intersection of foliation planes in high strain environment and that does not parallel the shear transport direction.

Shear zones in Ordovician granodiorites produced an anastomosing network that is centimeters to tens of meters in width (Simpson, 1983). In the study area (Roses, CDC3), the mylonitic foliation is inclined at 30–40° to the NE, parallel to the shear zone boundaries (Fig. 4c). Magnetic fabrics in the granodiorite have different characteristics. Similar to the Cap de Creus schists, a magnetic foliation defined by K_{max} and K_{int} roughly parallels the shear zone, which is oriented NW–SE and dipping about 40° to the NE. However, the K_{max} axes cluster along a NW–SE direction that corresponds to the stretching direction defined by a mineral elongation. Thus, the magnetic

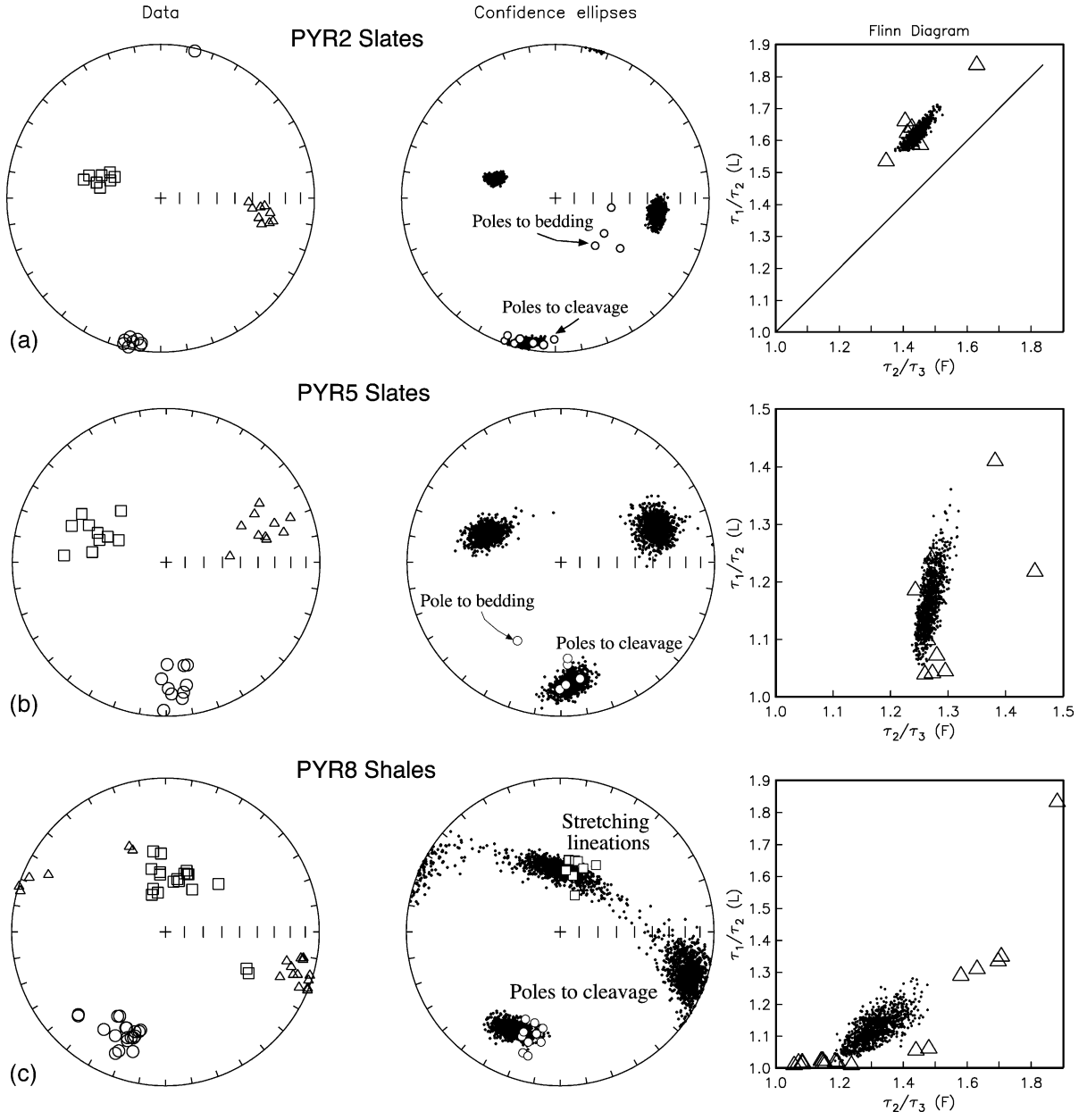

Fig. 3. Anisotropy of Magnetic Susceptibility data from PYR slates (Table 1) in the Central Pyrenees. On the left are equal area lower hemisphere projections of the principal (squares), major (triangles) and minor (circles) eigenvectors. To the right are bootstrapped eigenvectors from the data shown on the left and major structural elements (poles to bedding and cleavage and stretching lineation where present). Notice that the distribution of the principal eigenvectors ($\sim K_{max}$) do not conform the bedding and cleavage intersection. See text for discussion. Column at right shows Flinn diagrams, including individual sample data (triangles) and the bootstrapped averages for the whole data set (dots).

lineation in this shear zone in granodiorite tracks the stretching direction. We propose that the absence of a regional, pre-mylonitic foliation in the granodiorite enables the orientation of K_{max} axes to parallel the extension direction, as opposed to schists in the mylonite zone where two fabrics are present.

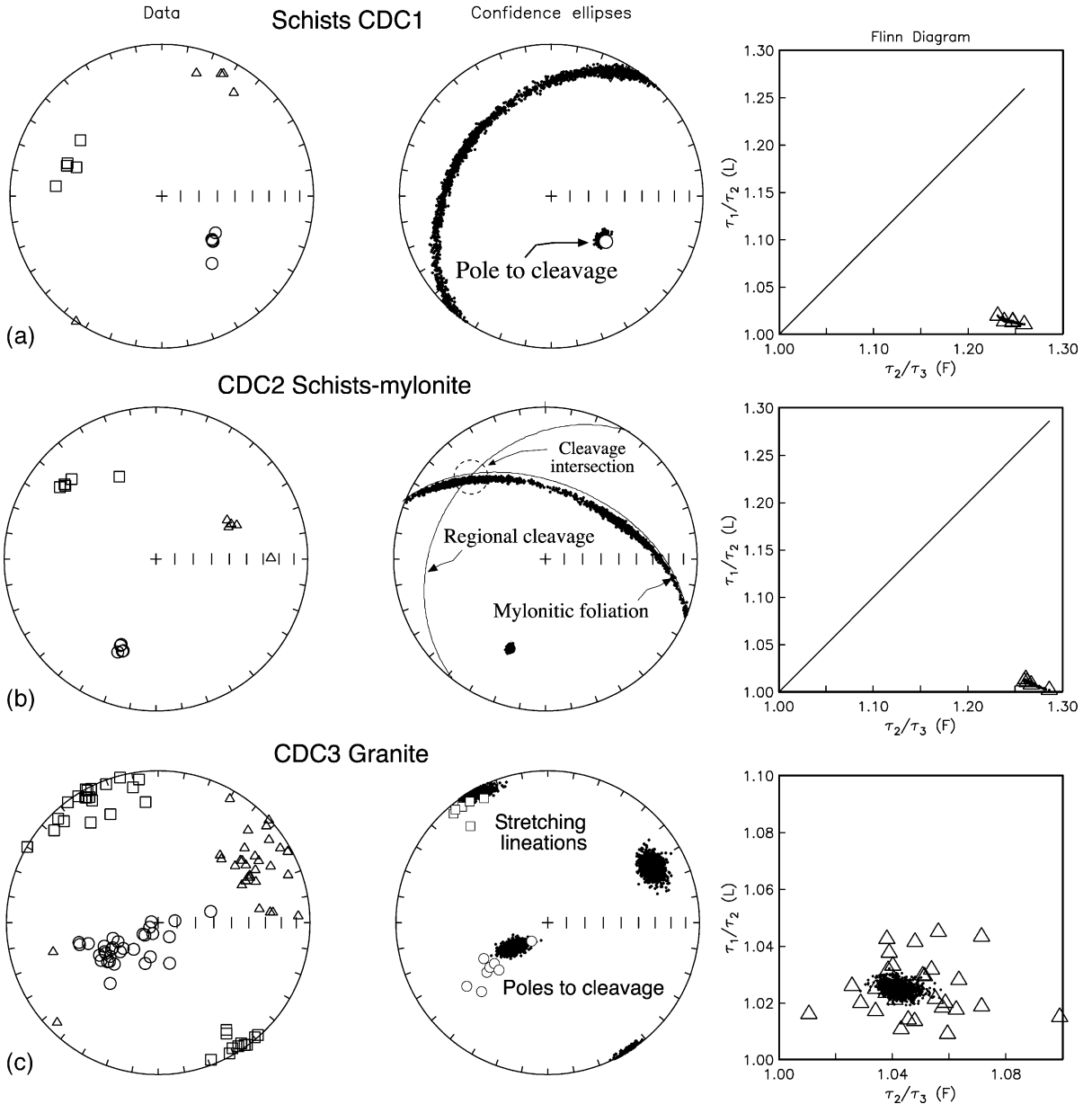

Fig. 4. Anisotropy of Magnetic Susceptibility data from CDC schist and granite in the Cap de Creus, Eastern Pyrenees. Same symbols as Fig. 2. The principal axes (squares) in the schist track the regional cleavage at locality CDC1 and the cleavage intersection direction in the mylonites at CDC2. Granite at locality CDC3 shows a magnetic lineation (grouping of K_{max}) that parallels the stretching direction as given by mineral elongation.

5.3. Pyrenean Foreland Basin mudrocks (sites FE)

In the Pyrenean Foreland Basin, a tectonic fabric due to N–S layer parallel shortening was progressively superimposed on a sedimentary fabric in flatlying mudrocks (Muñoz et al., 1999; Parés et al., 1999). The first evidence for the N–S shortening is the grouping of the principal axes of maximum suscept-

ibility parallel to the intersection of bedding and tectonic flattening plane (E–W direction). This result agrees with observations by Kissel et al. (1986) that were described in the previous section. This incipient deformation stage is characterized by grouping of the maximum susceptibility axis and preservation of the minimum axis normal to bedding. The minimum axes show a moderate/strong cluster on a stereonet projec-

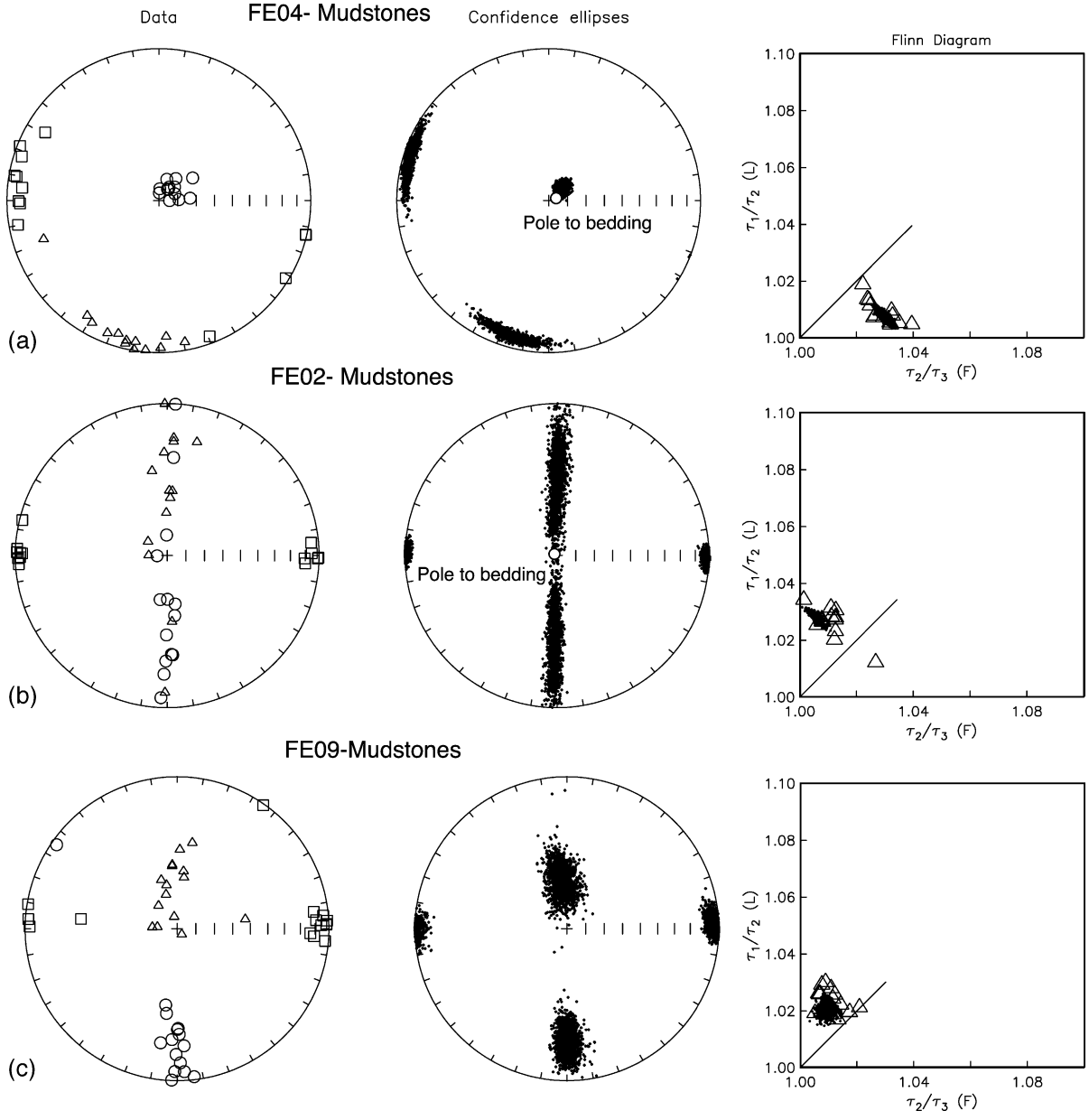

Fig. 5. Anisotropy of Magnetic Susceptibility data from FE mudstones in the Pyrenean Foreland Basin, Southern Pyrenees (Table 1). Same symbols as Fig. 3. The different stages of fabric development reflect a process of increasingly preferred re-orientation of phyllosilicates. In all cases, the maximum susceptibility axes parallel the bedding and flattening plane intersection.

tion (Fig. 5a). Close to the Pyrenean Fold and Thrust Belt, prolate magnetic ellipsoids develop, where the maximum axes are grouped parallel to the E–W direction and the minimum axes are distributed along a moderate girdle (Parés et al., 1999) (Fig. 5b,c). The preferred orientation of phyllosilicate grains causes a girdle distribution of the minimum and intermediate susceptibility axes parallel to Z and maximum direc-

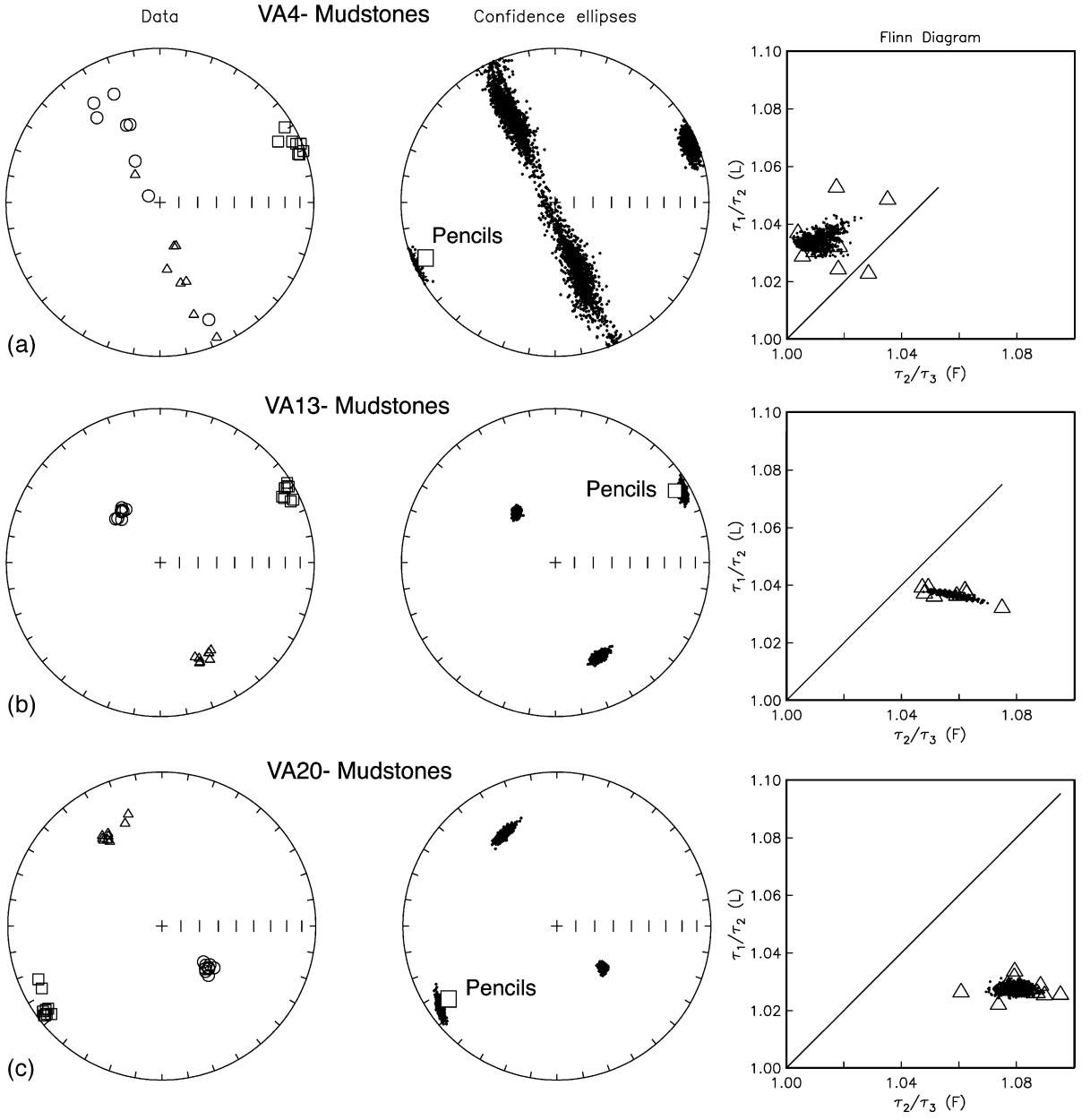

Fig. 6. Anisotropy of Magnetic Susceptibility data for pencil samples of the Knobs Formation, Valley and Ridge Province. Same symbols as Fig. 3. Squares indicate the orientation of the long axis of the pencils measured in the field.

tions are well clustered. This fabric progression records the competition between sedimentary and tectonic fabrics contributions, where the maximum susceptibility is parallel to the intersection of the flattening plane and bedding.

5.4. Knobs Formation pencils (sites VA)

Samples from Knobs Formation typically show a well-defined triaxial magnetic ellipsoid. Occasionally, the principal axes of susceptibility produce girdles, as opposed to the previous examples. Fig. 6 shows three different sites of mudstones with pencils, which are the product of bedding and cleavage intersection. In some cases, the pencils reach ratios length/width of 19 (Reks and Gray, 1982). However, no correlation between sizes or shape of pencils with magnetic fabric has been observed. Conversely, the long axis direction of pencils is always parallel to the maximum susceptibility axes K_{max}, whereas the minimum axes are normal to the bedding plane.

6. Discussion

Several variables govern the orientation of magnetic lineation in rocks, of which deformation intensity is an important, but not necessarily critical factor in determining the development of L_m. To illustrate the relationship between AMS and intensity of preferred orientation, a plot relating degree of anisotropy (P) and the degree of grain alignment is used (Fig. 7). Progressive grain re-orientation and its effect on the magnetic anisotropy is simulated by the anisotropic properties of a single crystalline grain, derived from a summation of the various orientations of individual grains (see Owens, 1974; Tarling and Hrouda, 1993; Hrouda and Schulmann, 1990 for details). Therefore, the degree of magnetic anisotropy of a rock whose anisotropy is carried by a single mineral provides an estimate of the degree of mineral alignment (Hrouda and Schulmann, 1990; Richter, 1992; Tarling and Hrouda, 1993). To first order, as the degree of strain increase, the intensity of preferred orientation in-

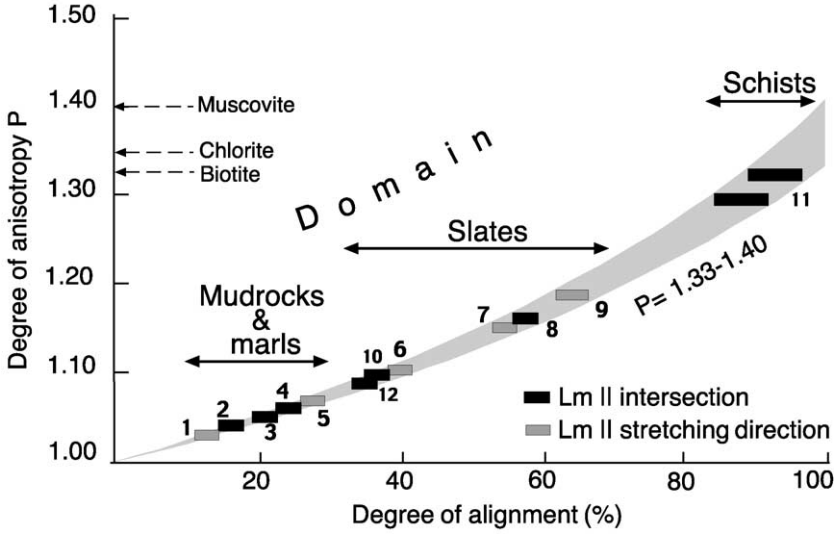

Fig. 7. Single-mineral model of rock magnetic anisotropy versus degree of mineral alignment (modified from Tarling and Hrouda, 1993). For a rock whose anisotropy is carried by a mineral with $1.33 < P < 1.40$, the degree of crystalline alignment can be directly determined from the degree of magnetic anisotropy P as indicated by the envelope (biotite: 1.33; chlorite: 1.36; muscovite: 1.40). Case studies include only pelitic and psammitic rocks, where phyllosilicates have been reported to be the main carriers of AMS and those where the anisotropy degree P has been calculated (or the necessary data to calculate it is provided): 1—Aubourg et al. (1991); 2—Pyrenean Foreland Basin mudrocks (Parés et al., 1999 and this study); 3—Sagnotti et al. (1999); 4—Sagnotti and Speranza (1993); 5—Mattei et al. (1999); 6—Lamarche and Rochette (1987); 7—Paleozoic slates with stretching lineation (PYR8, this study); 8—Paleozoic slates (PYR2 to 7, this study); 9—Hirt et al. (2000); 10—Knobs Formation pencils (VA7,8,13 and 20, this study); 11—Cap de Creus mylonites (CDC1 and 2, this study); 12—Lüneburg et al. (1999).

creases and hence, a plot of P versus degree of alignment offers a basis to compare relative deformation intensity (Fig. 7).

Since most iron phyllosilicates have very similar crystalline anisotropies ($1.33 < P < 1.40$), we use a single envelope that represents minerals with P from 1.33 to 1.40. This includes muscovite ($P = 1.40$), chlorite ($P = 1.36$) and biotite ($P = 1.33$) (Tarling and Hrouda, 1993); as shown in Fig. 7. The degree of alignment in a given rock cannot exceed the magnetic value when all grains of that mineral are perfectly aligned. For example, a rock whose magnetic fabric is solely due to muscovite will attain a maximum anisotropy degree P of 1.40 when all muscovite grains are perfectly aligned. The model that we use is thus valid for the case of a rock whose AMS carriers have $1.33 < P < 1.40$ that deforms under conditions obeying the March model. We note that numerical simulations of the magnetic fabric for both March and Jeffrey are quite similar (Richter, 1992). One aspect that could limit the use of the anisotropy degree as a deformation intensity gauge is change in magnetic mineralogy. Notably, changes in the amount of high susceptibility grains, like magnetite, introduce large changes in magnetic anisotropy (e.g. Borradaile, 1988). We have carried out a set of Low-Temperature experiments to determine the relative content of the ferromagnetic and paramagnetic components (Richter and van der Pluijm, 1994; Parés et al., 2000) (Fig. 8). The results indicate that only a minor contribution of ferromagnetism is present in slates. Most of the magnetic anisotropy is paramagnetic, as shown by the increase of bulk susceptibility at low temperature, validating our approximation of quantifying the preferred grain orientation using the increase of the magnetic anisotropy degree as shown in Fig. 7. In addition, we have not observed any dependence between the magnetic parameters (L, F) on the bulk susceptibility, which would suggest mineral changes as responsible for variations in magnetic anisotropy.

We have plotted on the envelope in Fig. 7 ($1.33 < P < 1.40$) the values of the anisotropy degree as observed in samples from a wide variety of deformation environments (see legend of Fig. 7 for sources). On the assumption that the AMS carriers for these rocks have similar P values (i.e. magnetic susceptibility due to biotite, muscovite or chlorite), the change in anisotropy degree provides a qualitative estimate

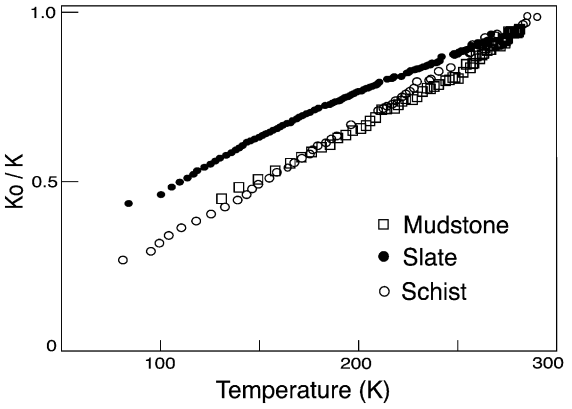

Fig. 8. Temperature dependence of low-field susceptibility for samples of selected lithologies, using the procedure of Richter and van der Pluijm (1994). K_0/K is the normalized reciprocal magnetic susceptibility (reading temperature during warming up versus ambient temperature, 290 K). The increase of the reciprocal susceptibility between 100 and 290 K indicates that samples are dominated by paramagnetic minerals.

of the degree of preferred orientation of the grains. As can be seen in Fig. 7, schists of the Cap de Creus shear zone show the highest degree of preferred orientation ($\sim 90\%$), whereas mudrocks result in very low anisotropies and thus low preferred orientation ($< 20\%$). Most importantly, Fig. 7 shows, however, that there is no unique correspondence between fabric intensity (as shown by preferred orientation intensity) and development of magnetic lineation. In mylonite and schists, having a degree of alignment of $\sim 90\%$ (Fig. 7), the magnetic lineation develops either parallel to the extension direction or is governed by the intersection between foliations. Similarly, in slates and mudrocks, the magnetic lineation is either parallel to the extension direction or to the intersection direction. Shales from the Knobs Formation with degree of alignment of $\sim 35\%$ and well developed pencil structure show a magnetic lineation that is consistent with such a fabric element, i.e. with the principal maximum susceptibility axes parallel to pencils.

Our results show that both magnitude and orientation of the pre-deformational AMS tensor control the development of magnetic fabric. Specifically two factors control the nature of L_m in deformed rocks: (1) the magnitude and orientation of the AMS original tensor, and (2) the magnitude and orientation of the

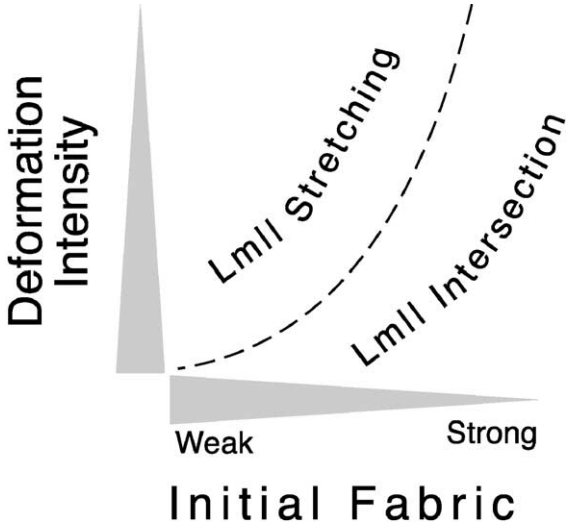

Fig. 9. Conceptual model of development of magnetic lineation with increasing deformation intensity. Horizontal axis is the degree of development or intensity of the initial (pre-deformational) magnetic fabric; vertical axis represents the deformation intensity. For rocks having a well-developed original AMS tensor, it will take significant finite strain to develop a magnetic lineation that parallels the finite stretching direction. When the original fabric is weak or absent, low deformation intensity will produce a magnetic lineation that tracks the extension direction.

finite strain. Fig. 9 is a conceptual representation that depicts the development of magnetic lineation as a function of the original AMS tensor and the deformation intensity. The practical implication of our study is that rocks with a relatively weak (pre-deformational) AMS tensor (e.g. granitoids, Bouchez, 1997) magnetic lineation will be highly sensitive to the extension direction of the finite strain. When an original fabric is well developed, however, the imprint of a second AMS tensor will produce a magnetic lineation that is in many cases parallel to the intersection direction (the angle between L_m and XY plane will be small) regardless of bulk finite strain of the rocks.

7. Conclusions

Our survey of magnetic fabrics in variably deformed rocks shows that the development of magnetic lineation, which is commonly parallel to the stretching direction or to the intersection of two fabrics, depends strongly on both the nature of an original fabric and the finite strain. For example, in highly strained, mylonitic gneisses, the magnetic lineation parallels the direction of transport, but in neighboring S–C mylonites, the lineation is perpendicular to this orientation. The variable orientation of the magnetic lineation, therefore, shows that magnetic fabrics cannot be used to track the finite strain ellipsoid, except in special circumstances. When more than one foliation is present in the deforming rock, as shown by this study, the magnetic lineation can be insensitive to finite strain. However, in rocks where pre-existing fabric is weak, like granitoid interiors, the magnetic fabric is dominated by the degree of deformation (e.g. Heller, 1973; Cogné and Perroud, 1988; Bouchez, 1997). In this environment, we can therefore use simple modeling approaches to quantify the deformation intensity, but elsewhere this approach is not reliable as a finite strain gauge.

Acknowledgements

This work was supported by the NSF Grant EAR9814343. The authors would like to thank G. Borradaile, B. Housen, K. Kodama, an anonymous reviewer and editor J.P. Burg for their comments on the manuscript. L. Holladay is acknowledged for laboratory assistance.

References

Aranguren, A., Cuevas, J., Tubia, J.M., 1996. Composite magnetic fabrics from S–C mylonites. J. Struct. Geol. 18, 863–869.

Aubourg, C., Rochette, P., Vialon, P., 1991. Subtle stretching lineation revealed by magnetic fabric of Callovian–Oxfordian black shales (French Alps). Tectonophysics 185, 211–223.

Borradaile, G., 1987. Anisotropy of magnetic susceptibility: rock composition versus strain. Tectonophysics 138, 327–329.

Borradaile, G.J., 1988. Magnetic susceptibility, petrofabrics and strain. Tectonophysics 156, 1–20.

Borradaile, G.J., 1991. Correlation of strain with anisotropy of magnetic susceptibility (AMS). Pure Appl. Geophys. 135, 15–29.

Borradaile, G.J., Henry, B., 1997. Tectonic applications of magnetic susceptibility and its anisotropy. Earth Sci. Rev. 42, 49–93.

Borradaile, G.J., Tarling, D.H., 1981. The influence of deformation mechanisms on magnetic fabrics in weakly deformed rocks. Tectonophysics 77, 151–168.

Bouchez, J.L., 1997. Granite is never isotropic: an introduction to AMS studies of granitic rocks. In: Bouchez, J.L., et al. (Eds.),

Granite: From Segregation of Melt to Emplacement Fabrics. Kluwer Academic Publishing, Rotterdam, pp. 95–112.
Capellà, I., 1997. Strain analysis in the Axial Zone of the Variscan basement of the Pyrenees. Geol. Mijnbouw 75, 361–371.
Carreras, J., Druguet, E., 1994. Structural zonation as a result of inhomogeneous non-coaxial deformation and its control on syntectonic intrusions: an example from the Cap de Creus area, eastern-Pyrenes. J. Struct. Geol. 16, 1525–1534.
Carreras, J., Estrada, A., White, S., 1977. The effect of folding on the *c*-axis fabrics of quartz mylonite. Tectonophysics 39, 3–25.
Casas, J.M., Durney, D., Ferret, J., Muñoz, J.A., 1996. Detrminación de la deformación finita en la vertiente sur del Pirineo oriental a lo largo de la transversal del rio Ter. Geogaceta 20, 803–805.
Casas, J.M., Parés, J.M., Megías, L., 1998. La fábrica magnética de los materiales cambroordovícicos de la parte oriental del anticlinal de La Massana (Andorra, Pirineo Central). Rev. Soc. Geol. España 11, 317–329.
Choukroune, P., ECORS team, 1989. The ECORS Pyrenean deep seismic profile reflection data and the overall structure of an orogenic belt. Tectonics 8, 23–39.
Cirès, J., Alías, G., Poblet, J., Casas, J.M., 1990. La estructura del anticlinal de la Massana. Geogaceta 8, 42–44.
Cogné, J.P., Perroud, H., 1988. Anisotropy of magnetic susceptibility as a strain gauge in the Flamanville granite, NW France. Phys. Earth Planet. Inter. 51, 264–270.
Constable, C., Tauxe, L., 1990. The bootstrap for magnetic susceptibility tensors. J. Geophys. Res. 95, 8383–8395.
Deramond, J., Graham, R.H., Hossak, J.R., Baby, P., Crouzet, G., 1985. Nouveau modéle de la chaine des Pyrénées. C. R. Acad. Sci. Paris 301, 1213–1216.
Druguet, E., Passchier, C.W., Carreras, J., Victor, P., den Brok, S., 1997. Analysis of a complex high-strain zone at Cap de Creus, Spain. Tectonophysics 280, 31–45.
Ferré, E.C., Améglio, L., 2000. Preserved magnetic fabrics vs. annealed microstructures in the syntectonic recrystallised George granite, South Africa. J. Struct. Geol. 22, 1199–1219.
Goldstein, A.G., 1980. Magnetic susceptibility anisotropy of mylonites from the Lake Char mylonite zone, southeastern New England. Tectonophysics 66, 197–211.
Goldstein, A.G., Brown, L.L., 1988. Magnetic susceptibility anisotropy of mylonites from the Brevard Zone, North Carolina, USA. Phys. Earth Planet. Inter. 51, 290–300.
Heller, F., 1973. Magnetic anisotropy of granitic rocks of the Bergell Masif (Switzerland). Earth Planet. Sci. Lett. 20, 180–188.
Hirt, A., Julivert, M., Soldevila, J., 2000. Magnetic fabric and deformation in the Navia–Alto Sil slate belt, northwestern Spain. Tectonophysics 320, 1–16.
Housen, B.A., van der Pluijm, B.A., 1990. Chlorite control of correlations between strain and anisotropy of magnetic susceptibilty. Phys. Earth Planet. Inter. 61, 315–323.
Housen, B.A., van der Pluijm, B.A., 1991. Slaty cleavage development and magnetic anisotropy fabrics (AMS and ARMA). J. Geophys. Res. 96, 9937–9946.
Housen, B.A., Richter, C., van der Pluijm, B.A., 1993. Composite magnetic anisotropy fabrics: experiments, numerical models, and implications for the quantification of rock fabrics. Tectonophysics 200, 1–12.
Housen, B.A., van der Pluijm, B.A., Essene, E.J., 1995. Plastic behaviour of magnetite and high strains obtained from magnetic fabrics in the Parry Sound shear zone, Ontario, Grenville Province. J. Struct. Geol. 17, 265–278.
Hrouda, F., 1982. Magnetic anisotropy of rocks and its application in geology and geophysics. Geophys. Surv. 5, 37–82.
Hrouda, F., Schulmann, K., 1990. Conversion of the magnetic susceptibility tensor into the orientation tensor in some rocks. Phys. Earth Planet. Inter. 63, 71–77.
Jelinek, V., 1976. The statistical theory of measuring anisotropy of magnetic susceptibility of rocks and its application, Brno. Geophysika, 1–88.
Jelinek, V., 1978. Statistical processing of anisotropy of magnetic susceptibility measured on groups of specimens. Stud. Geophys. Geol. 22, 50–62.
Kissel, C., Barrier, E., Laj, C., Lee, T.Q., 1986. Magnetic fabric in 'undeformed' marine clays from compressional zones. Tectonics 5, 769–781.
Kligfield, R., Owens, W.H., Lowrie, W., 1981. Magnetic susceptibility anisotropy, strain and progressive deformation in Permian sediments from the Maritime Alps (France). Earth Planet. Sci. Lett. 55, 181–189.
Lamarche, G., Rochette, P., 1987. Microstructural analysis and origin of lineations in the magnetic fabric of some Alpine slates. Tectonophysics 139, 285–293.
Lüneburg, C.M., Lampert, S.A., Lebit, H.D., Hirt, A.M., Casey, M., Lowrie, W., 1999. Magnetic anisotropy, rock fabrics and finite strain in deformed sediments of SW Sardinia (Italy). Tectonophysics 307, 51–74.
Mattei, M., Speranza, F., Argentieri, A., Rossetti, F., Sagnotti, L., Funiciello, R., 1999. Extensional tectonics in the Amantea basin (Calabria, Italy): a comparison between structural and magnetic anisotropy data. Tectonophysics 307, 33–49.
Muñoz, J.A., Martínez, A., Vergés, J., 1986. Thrust sequences in the Spanish eastern Pyrenees. J. Struct. Geol. 8, 399–405.
Muñoz, J.M., Casas, J.M., Parés, J.M., Durney, D., 1999. Internal deformation related to thrust evolution in the Eastern Pyrenees. Thurst Tectonics Meeting, Royal Holloway University of London.
Nye, J.F., 1957. The Physical Properties of Crystals. Clarendon Press, Oxford, 322 pp.
Owens, W.H., 1974. Mathematical model studies on factors affecting the magnetic anisotropy of deformed rocks. Tectonophysics 24, 115–131.
Parés, J.M., Dinarès, J., 1993. Magnetic fabric in two sedimentary rock types from the Southern Pyrenees. J. Geomagn. Geoelectr. 45, 193–205.
Parés, J.M., van der Pluijm, B., Dinarès-Turell, J., 1999. Evolution of magnetic fabrics during incipient deformation of mudrocks (Pyrenees, northern Spain). Tectonophysics 307, 1–14.
Parés, J.M., van der Pluijm, B.A., Holladay, L., 2000. Low-temperature of the anisotropy of magnetic susceptibility. AGU Fall Meeting, San Francsico, California.
Piazolo, S., Passchier, C.W., 2002. Controls on lineation development in low to medium grade shear zones: a study from the Cap de Creus peninsula, NE Spain. J. Struct. Geol. 24, 25–44.
Poblet, J., 1991. Estructura hercínica i alpina del vessant Sud de la

zona axial del Pirineu central. PhD Diss., Universitat de Barcelona, 604 pp.

Reks, I., Gray, D., 1982. Pencil structure and strain in weakly deformed mudstone and siltstone. J. Struct. Geol. 4, 161–176.

Richter, C., 1992. Particle motion and the modelling of strain response in magnetic fabrics. Geophys. J. Int. 110, 451–464.

Richter, C., van der Pluijm, B.A., 1994. Separation of paramagnetic and ferrimagnetic susceptiblities using low temperature magnetic susceptiblities and comparison with high field methods. Phys. Earth Planet. Inter. 82, 113–123.

Richter, C., van der Pluijm, B.A., Housen, B.A., 1993. The quantification of crystallographic preferred orientation using magnetic anisotropy. J. Struct. Geol. 15, 113–116.

Rochette, P., Vialon, P., 1984. Development of planar and linear fabrics in Dauphinois shales and slates (French Alps) studied by magnetic anisotropy and its mineralogical control. J. Struct. Geol. 6, 33–38.

Ruf, A.S., Naruk, S.J., Butler, R.F., Calderone, G.J., 1988. Strain and magnetic fabric in the Santa Catalina and Pinaleno mountains metamorphic core complex mylonite zones, Arizona. Tectonics 7, 235–248.

Sagnotti, L., Speranza, S., 1993. Magnetic fabrics analysis of the Plio–Pleistocene clayey units of the Sant'Arcangelo basin, Southern Italy. Phys. Earth Planet. Inter. 77, 165–176.

Sagnotti, L., Faccenna, C., Funiciello, R., Mattei, M., 1994. Magnetic fabric and structural setting of Plio–Pleistocene clayey units in an extensional regime: the Tyrrhenian margin of central Italy. J. Struct. Geol. 16, 1243–1257.

Sagnotti, L., Winkler, A., Montone, P., Di Bella, L.D., Florindo, F., Mariucci, M.T., Marra, F., Alfonsi, L., Frepoli, A., 1999. Magnetic anisotropy of Plio–Pleistocene sediments from the Adriatic margin of the northern Apennines (Italy): implications for the time–space evolution of the stress field. Tectonophysics 311, 139–153.

Seguret, M., 1972. Étude tectonique des nappes et séries décollées de la partie centrale du versant sud des Pyrénées. Pub. Ustela, Sér., Geol. Struct., Montpellier 2, 1–155.

Simpson, C., 1983. Displacement and strain patterns from naturally occurring shear zone terminations. J. Struct. Geol. 5, 497–506.

Simpson, C., Carreras, J., Losantos, M., 1982. Inhomogeneous deformation in Roses granodiorite, NE Spain. Acta Geol. Hisp. 17, 219–226.

Tarling, D.H., Hrouda, F., 1993. The Magnetic Anisotropy of Rocks. Chapman & Hall, London, 217 pp.

Tauxe, L., 1998. Paleomagnetic Principles and Practice. Kluwer Academic Publishers, Dordrecht, 299 pp.

Tikoff, B., Greene, D., 1997. Stretching lineations in transpressional shear zones: an example from Sierra Nevada Batholith, California. J. Struct. Geol. 19, 29–39.

Zwart, H.J., 1979. The geology of the Central Pyrenees. Leidse Geol. Meded. 50, 1–74.